photonics

MDPI

Article

Theoretical Substantiation of the Possibility of Performing Non-Damaging UV Diagnostics of Biological Tissues In Vivo

Andrey P. Tarasov [1,2,*], Maria E. Shtyflyuk [1] and Dmitry A. Rogatkin [1]

[1] Moscow Regional Research and Clinical Institute ("MONINI"), 129110 Moscow, Russia
[2] Shubnikov Institute of Crystallography, Federal Scientific Research Centre "Crystallography and Photonics", Russian Academy of Sciences, 119333 Moscow, Russia
* Correspondence: tarasov.ap@phystech.edu

Abstract: Since UV radiation is capable of causing skin erythema, there is a risk of damage during in vivo UV spectroscopy of skin. In particular, the conventional estimation of radiation dose indicates the impossibility of conducting such studies when using fiber sources to deliver UVA and UVB radiation to the skin due to the rapid accumulation of the minimal erythema dose (MED). Using numerical simulations, we investigated the possibility of achieving MED when exposing the skin to UV light of diagnostic power and forming irradiation spots of different sizes. It has been shown that the conventional approach to calculating the dose as radiant exposure (J/cm^2) turns out to be unsuitable in the case of irradiation spots of small area (which is the case when fiber sources are used) since it greatly overestimates the dose. This, in turn, results in a significant underestimation of the permissible duration of the diagnostic procedure. The reason for this is the failure to take into account the diffusion of radiation in biological tissue. We substantiated that for a more correct calculation of the dose taking into account diffusion, it is necessary to estimate the volumetric energy density (J/cm^3) in biological tissue. In vivo experiments confirmed that this approach is more correct in determining the time to reach erythema compared to the conventional approach. The calculations showed that the minimum spot area of UVA/UVB irradiation on the skin surface, beyond which the calculation of the dose as radiant exposure does not introduce a significant error, is 1.5–3 mm^2, which corresponds to diameters of 1.4–2 mm in the case of a round irradiation spot.

Keywords: erythema; minimal erythema dose; ultraviolet; diagnostics; UV damage; UV absorption; skin; Monte Carlo simulations; fiber optics; energy density

Citation: Tarasov, A.P.; Shtyflyuk, M.E.; Rogatkin, D.A. Theoretical Substantiation of the Possibility of Performing Non-Damaging UV Diagnostics of Biological Tissues In Vivo. *Photonics* **2023**, *10*, 1289. https://doi.org/10.3390/photonics10121289

Received: 16 October 2023
Revised: 16 November 2023
Accepted: 20 November 2023
Published: 22 November 2023

1. Introduction

Despite the rich history of the application of light in medicine, numerous studies of mechanisms of radiation effects on biological tissues, the development of artificial light sources and measuring equipment, as well as many issues of optical radiation dosimetry, especially in the ultraviolet (UV) range, are still relevant today. Moreover, when there is a need to describe the impact of UV radiation on biological objects, specialists face a number of ambiguities and uncertainties, which are only partially offset by existing manuals on dosimetry and calibration in phototherapy [1,2].

UV radiation is actively applied in the clinic as a physical therapeutic and prophylactic agent, due to a number of positive biological effects (immunomodulatory, anti-inflammatory, bactericidal, etc.). In dermatology, UV light is widely used in the diagnosis and phototherapy of various skin pathologies. However, excessive UV exposure can cause acute and long-term negative effects. The photodestructive effect of UV radiation on a cell is similar to the effect of ionizing radiation: DNA structure damage, photoinactivation of proteins, changes in ion permeability, damage to cell membrane systems, etc. Fatal cell damage or failure in cell repair mechanisms leads to the triggering of apoptosis, necrosis or mutagenesis [3].

In the arsenal of doctors, researchers and medical physicists working with ionizing radiation, there is a clearly defined glossary for describing the physical and biological effects of the interaction of ionizing radiation with biological tissues, as well as a number of standards, protocols and recommendations in the field of dosimetry, e.g., IAEA TRS 398 [4] and AAPM TG 51 [5]. In particular, the following quantities are used to describe and characterize radiation doses: exposure dose (C/kg), which reflects ionization effects in air; absorbed dose ((J/kg) or (Gy)), which characterizes the absorbed energy in a substance; and equivalent and effective doses, which take into account differences in the damaging effects of various particles, as well as the susceptibility of various organs to radiation. Such an approach allows one to wholly consider the dose–response relationship, assessing both the amount of energy absorbed by the sensitive volume of the substance and the features of the interaction of this type of radiation with the irradiated matter.

In contrast, the dose of UV radiation affecting living tissue is usually measured in units of radiant exposure or fluence—the incident radiation energy per unit area of a tissue (J/m^2). However, this value rather denotes the surface density of the incident energy and in no way reflects the processes occurring inside the tissue. Taking into account the fact that the penetrating ability of UV radiation at different wavelengths is not the same, and the variability of tissue characteristics significantly affects the propagation of radiation inside the tissue, it is difficult to assess the severity of damage caused by UV radiation using only this value. Moreover, when choosing doses for phototherapy, it is necessary to rely on the individual response of the patient's skin to the UV radiation of a selected source.

To date, in dermatology, the only generally accepted objective measure of skin response sensitivity to UV exposure is the minimal erythema dose (MED). This is the surface energy density (J/m^2) that corresponds to the formation of minimally distinguishable erythema when skin is exposed to UV radiation for a certain time. In clinical practice, this value is determined individually, by test irradiation of small equal areas of skin with different stepwise-increasing doses. In phototherapy, light from the spectral range of 310–315 nm is widely used: NB-UVB phototherapy with an emission peaking at 310–311 nm; targeted therapy with an excimer laser (308 nm). The UVA range is also often used: UVA therapy (320–340 nm) and PUVA therapy (combined use of a photosensitizing drug from the psoralens group and irradiation in the UVA range) [2]. Typically, MEDs for fair skin types that are more sensitive to the harmful effects of UV radiation (Fitzpatrick phototypes I and II) are in the order of 1 J/cm^2 for narrowband UVB [6], and tens of J/cm^2 for UVA sources [7]. As a rule, suberythemal doses are used for phototherapy since the formation of erythema itself indicates the triggering of inflammatory reactions in response to cell necrosis. Therefore, exceeding the MED is undesirable.

In addition to therapeutic techniques, optical methods for diagnostic purposes have been extensively developed, allowing non-invasive in vivo evaluation of the optical properties of biological tissues [8]. For this purpose, UV radiation can also be used [9–11]. Some of them are based on measurements using fiber optic probes [12]. In this case, the delivery of diagnostic UV radiation to the tissue is also carried out using optical fibers. Simple calculations show that when the skin is exposed to milliwatt-power UV radiation emitted by an optical fiber with a diameter of, for example, 100 microns, the MED value is exceeded even with a short-term exposure of a few seconds. However, from our practice with fiber optic diagnostic equipment in the UV range, the formation of erythema is not observed even during minutes of exposure [13]. To the best of our knowledge, there are no such reports about erythema formation from other researchers.

Thus, the following question arises: How legitimate is it to define the concept of "radiation dose" in terms of radiant exposure (J/cm^2) in relation to fiber optic diagnostic procedures or, in general, in the case of small spots of UV irradiation formed on the skin? In this regard, the goal of this study is to theoretically investigate the distribution of absorbed UV light in skin in the case of the formation of irradiation spots of various sizes on the skin surface and evaluate the absorbed radiation in comparison with known data on MEDs, estimating both surface and volume energy density. Herewith, the cases of different UV

ranges are of interest due to the significant difference in the MED values. In this study, we consider UVA and UVB light. The results obtained were verified in an in vivo experiment to determine the time to reach erythema during irradiation with a fiber source.

2. Materials and Methods

2.1. Research Outline

The study was carried out in 4 stages. In Stage I, the diffuse reflection of UV radiation from the skin of the forearms of Caucasian volunteers with Fitzpatrick phototype II was experimentally measured. The measurements were carried out for two different wavelengths, 337 (UVA) and 315 nm (UVB), using a fiber probe of the Multicom system described below (see Section 2.2). The distal end of the fiber was in close contact with the skin. The diffuse reflectance data obtained in the previous stage were then used in Stage II, where the optical parameters of the skin were sought at selected wavelengths using Monte Carlo (MC) simulations of light propagation in biological tissues. Stage III was the main one in this work. It was devoted to the MC calculations of the distribution of the absorbed radiation energy in skin using the optical parameters found in Stage II. Calculations were carried out for different sizes of irradiation spots on the skin surface. The goal of this stage was to determine the effect of diffusion of light on the size of the tissue region in which it is absorbed, and thus to understand in which cases it is necessary to take light diffusion into account when estimating the absorbed fraction of radiation. Finally, Stage IV had as its main task checking the validity of the results and conclusions obtained in the previous stages and their usefulness in a real experiment in terms of assessing the MED and the permissible time for the diagnostic procedure. To evaluate whether the MED was exceeded, two different approaches were applied to calculate doses. In the first case, a dose D_S was calculated as radiant exposure:

$$D_S = \frac{P \cdot t}{S} \left[\mathrm{J/cm^2} \right], \tag{1}$$

where S is an area ($\mathrm{cm^2}$) of a light spot on a skin surface (or area of an emitting surface of a light source if it is in direct contact with skin—this is a case when a fiber source is used), t is the exposure time and P is a power (W) of incident light in this spot (so, $P \cdot t$ is the incident energy). This approach of dose calculation can be called a conventional or surface approach.

Within a second approach, called a volumetric approach, a dose was calculated as the energy per certain volume V_α, in which a part equal to α of all absorbed radiation was accumulated:

$$D_V = \alpha A \frac{P \cdot t}{V_\alpha} \left[\mathrm{J/cm^3} \right], \tag{2}$$

where A is all energy absorbed in tissue as a fraction of incident radiation. Thus, $\alpha \cdot A \cdot P \cdot t$ is energy absorbed in a volume V_α. The shape of this volume is determined only by a condition that α-portion of all absorbed radiation ($A \cdot P \cdot t$) is concentrated in this volume—so, its projection to the tissue surface can be larger than the source diameter due to light diffusion in a tissue. In this research, we take $\alpha = 0.95$.

To compare calculated values for D_V with the *MED*, the *MED* value $D_{S,MED}$ known from the literature was expressed in the units of $\mathrm{J/cm^3}$, giving $D_{V,MED}$. In our study, we used the MED values equal to 0.87 $\mathrm{J/cm^2}$ for UVB and 23.8 $\mathrm{J/cm^2}$ for UVA as obtained in [14]. Based on the data obtained, the time required to achieve MED was estimated within the framework of the conventional surface approach, operating with $D_{S,MED}$, and the volumetric approach, which involves calculating $D_{V,MED}$. The obtained time values were compared with the results of the experiment, where the time to reach erythema was estimated. Irradiation was carried out using a fiber probe of the Multicom system. The distal end of the fiber was in close contact with the skin. Erythema was recorded visually 24 h after irradiation on the forearm of a healthy volunteer with Fitzpatrick phototype II.

2.2. Experimental

In the experimental part of the research, a non-commercial multifunctional Multicom system previously developed for in vivo optical spectroscopy [15] was used. Figure 1 shows a schematic representation of three main optical units of this system—a fiber probe, light source(s) and a spectrometer. The distal end of the fiber probe contains one central receiving fiber with a diameter of 400 μm, located in the center of a large number of emitting fibers with a diameter of 100 μm, 19 of which are used for the UV radiation source to deliver the radiation to the skin. A large number of emitting fibers allows one to distribute the dose exposure over the skin surface, to decrease the influence of skin inhomogeneities on diagnostic results. Thus, in our study, 19 emitting fibers for UV radiation were used (the total area is ~$14.9 \cdot 10^{-4}$ cm^2 for all 19 fibers). The distance between the centers of the receiving and emitting fibers is 1.05 mm. The receiving fiber is connected to the spectrometer.

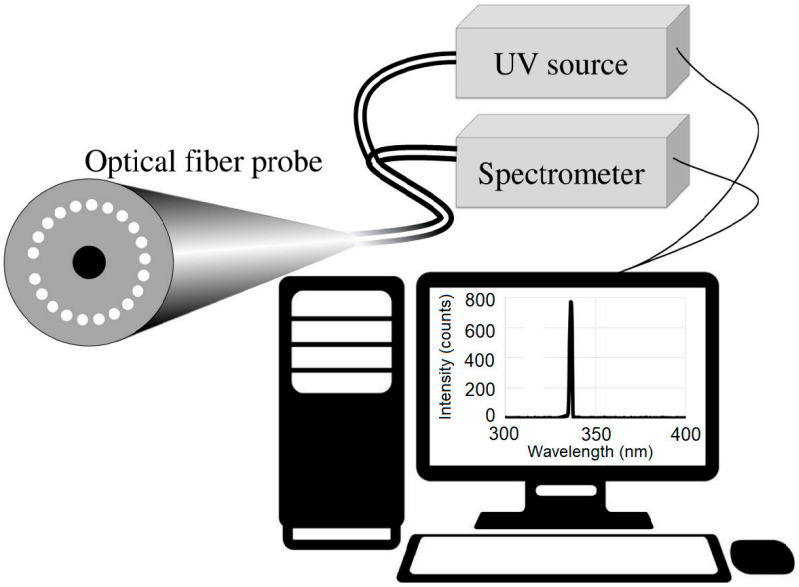

Figure 1. A schematic diagram of main components of the Multicom system.

The measurements of diffuse reflectance (relative backscattered flux) were performed at two wavelengths: 337 nm and 315 nm. The light with λ = 337 nm was emitted by a pulsed nitrogen laser with a pulse frequency of ~100 Hz. The *cw* xenon lamp was used to obtain emission with λ = 315 nm. To select this wavelength, UVG-2 (UFS-2) and YGG-3 (ZhS-3) optical filters were mounted sequentially at the output window of the lamp. This allows obtaining an emission band with a maximum at 315 nm, a full width at half maximum of ~20 nm, and a shape close to Gaussian. The light emitted by the laser and the lamp was delivered to the skin by the fiber probe described above. The average power of emission with λ = 337 nm at the distal end of the fiber probe was 2.31 mW as measured by an Ophir power meter with PD-10C and PE-10 measuring head. In the case of a 315 nm emission band, the power was ~70 μW, as was measured using a reflectance standard Spectralon (Labsphere Ltd., North Sutton, NH, USA) with a technique described in [16], taking into account the spectral width of the band.

2.3. Monte Carlo Modeling

The Monte Carlo (MC) method was applied for 3D simulations of the propagation of UV radiation in skin. The weighted photon model was implemented in MC to account for absorption, which is often used for MC simulations in biomedical photonics [17,18]. To describe light scattering, the Henyey–Greenstein phase function with the anisotropy factor *g* was used. The skin model is a heterogeneous medium with two flat layers, modeling the epidermal and dermal layers of skin. The thickness of the first layer was taken to be

100 μm [19], whereas the second layer was semi-infinite (this does not affect the reliability of the simulation results, since UV radiation does not penetrate deep into the skin). To model incident radiative flux, 10^7–10^8 (depending on the particular task) photon packets were launched in simulations. The MC simulations were performed using Matlab R2022a software (ver. 9.12.0.1975300, MathWorks, Natick, MA, USA).

The MC modeling was implemented for both wavelengths used in experiments (337 nm and 315 nm). The selection of the optical parameters of the skin layers (the absorption coefficient μ_a, the reduced scattering coefficient μ_s', g and the refractive index n) for the model was first carried out on the basis of literature data. The g factor and the refractive index n were assumed to be 0.7 and 1.4, respectively, for both layers [20].

In MC modeling in Stage II, the angular aperture of a receiving fiber with a diameter of 400 μm was taken equal to 20° (as for emitting fibers with a diameter of 100 μm) in accordance with the technical characteristics of the probe used in the in vivo experiments. The refractive index of the fibers' core was taken to be 1.4; so, a reflection-index-matched boundary condition takes place in the case of a contact of a fiber probe with skin. To eliminate the influence of the statistical error on the simulation results, a relative backscattered flux (the ratio of backscattered and tissue-incident fluxes) was calculated for a set of different distances between the centers of the emitting and receiving fibers (source–detector distance (SDD)). SDDs from 0.4 to 1.2 mm in 50 μm increments were modeled. This set includes SDD = 1.05 mm, corresponding to the actual distance in the optical probe used. To match the experiment, a simulated backscattered flux registered by the receiving fiber was multiplied by 19, corresponding to the number of emitting fibers. In addition, the total transmittance of the epidermal layer $T_{epidermis}$ and the total diffuse reflectance R_{skin} of the skin were used as additional reference parameters to narrow the range of possible μ_a and μ_s' values. In MC simulations, $T_{epidermis}$ and R_{skin} values were maintained at the level of 10–15% [19,21].

Using the optical parameters found in Stage II, the distribution of the absorbed radiation energy in the skin was calculated in Stage III. To do this, a grid was created in the two-layer tissue model, each element of which was a cubic voxel with a side size of 10 μm. To clarify the effect of diffusion of light in tissue, a series of model experiments were carried out with different sizes of a circular irradiation spot with a diameter d (and area S), which varied from 10 μm to 4 mm with different steps (depending on the significance of the simulated interval of d). In particular, d = 100 μm corresponds to the case of a fiber optic source, which we use in our work, including this study. The geometric center of the irradiation spot in the model was at $x = 0$, $y = 0$, $z = 0$; the Z axis represents the direction to the depth of the skin.

3. Results and Discussion

3.1. Determination of Diffuse Reflectance from Skin

An experimental study of the diffuse reflectance using a fiber probe of a Multicom system (SDD = 1.05 mm) showed that in the case of light with wavelengths of 337 nm and 315 nm, a receiving fiber registered on average $8.6 \cdot 10^{-8}$ and $1.7 \cdot 10^{-8}$ of the incident power, respectively. These values were used further in MC computations.

3.2. Selection of the Optical Parameters of Skin

In the literature, one can find a rather huge scatter of data on μ_a and μ_s' for skin and its layers, including those for UV. However, as it was determined, many of them lead to significant discrepancies with the experimental results obtained in our experiment, underestimating the backscattering fluxes in most cases. Eventually, when selecting optical parameters using MC modeling, we used the data on the optical properties of the skin given in [22,23] as they allowed us to obtain results closer to the experimental ones as compared to other literature data. Also, we relied on data on the absorption of UV light by blood and melanin [24,25]. Next, the optical parameters were varied (with an increment of 5 cm^{-1}) in the course of solving the direct problem of light propagation by the MC method

until the backscattered flux values observed in the experiments were achieved, maintaining the $T_{epidermis}$ and R_{skin} values in the range of 10–15%. The finally chosen pairs of μ_a and μ_s' values used further to calculate absorption in skin are shown in Table 1.

Table 1. Selected absorption μ_a and scattering μ_s' coefficients of the epidermal and dermal layers.

Layer	μ_a (cm^{-1})/μ_s' (cm^{-1})	
	λ = 337 nm	**λ = 315 nm**
Epidermis	80/120	100/125
Dermis	30/115	35/120

Figure 2 shows the relative backscattered flux for two chosen wavelengths and various SDD values. In particular, at SDD = 1.05 mm, we obtain a relative flux of ~$8.6 \cdot 10^{-8}$ for λ = 337 nm and $1.7 \cdot 10^{-8}$ for λ = 315 nm, which corresponds to experimental data.

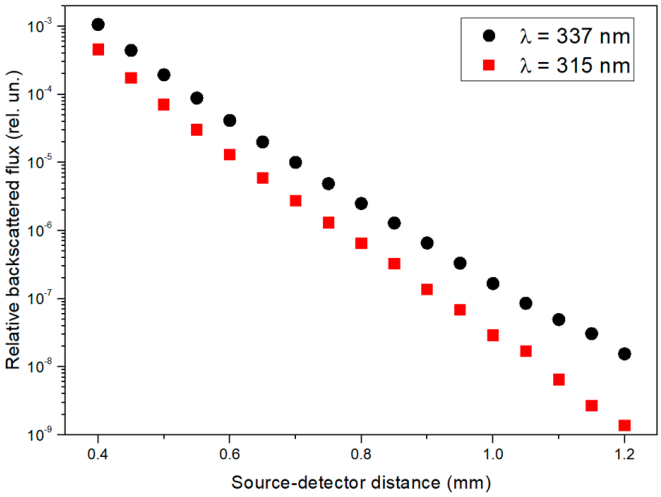

Figure 2. Relative backscattered fluxes vs. SDD calculated by MC simulations in the 2-layer model of skin at λ = 337 nm (black circles) and 315 nm (red squares) for optical fiber probe (d = 100 μm) as a light source.

3.3. Calculation of Distribution of Radiation Energy Absorption in Skin

Figure 3 shows as an example the calculated distributions of absorbed UVA radiation (λ = 337 nm) in a model two-layer medium in two different cross-sections of the medium (one layer of voxels). The cases of two significantly different diameters of the irradiation spot are shown: d = 100 μm (Figure 3a,b) and d = 3 mm (Figure 4). The strength of absorption in different areas of the medium (sometimes also called the absorbed fraction), represented by the normalized photon weight that was absorbed, is shown in a logarithmic scale by different colors in accordance with the color bar. The intensity in each voxel is normalized to the maximum energy absorbed in the cross-section. The vertical axis (Z) is the depth (cm), and the horizontal axis (X) is the distance (cm) in the lateral direction.

In particular, the absorption distribution shown in Figure 3a corresponds to the cross-section drawn through the central axis of the irradiation spot with d = 100 μm (axially symmetric image). Taking into account the simulation parameters, this case can be considered as modeling the UV irradiation of skin by an optical fiber. It can be seen that the maximum absorption occurs directly in the area under the irradiation spot. The difference in absorption in the first and second layers is also clearly seen. It is provided by the significant difference in the absorption coefficient μ_a of the layers. At the depth of ~0.7 mm, corresponding to the second layer, the absorption is already ~10^5 times lower than that in the first layer in the region directly under the irradiation spot. Figure 3b shows the distribution of absorbed radiation in a cross-section 0.75 mm away from the center of the irradiation spot (or from the central cross-section in Figure 3a), which corresponds to the

lateral coordinate $y = 0.75$ mm. In this region far from the irradiation spot (and, accordingly, collimated radiation), the process of light diffusion plays a more noticeable role. Owing to it, the absorption is much more uniformly distributed over this cross-section and shows smaller variations at large distances compared to the area directly under the irradiation spot. In addition, the region of maximum absorption is shifted deeper down ($z \sim 0.3$ mm).

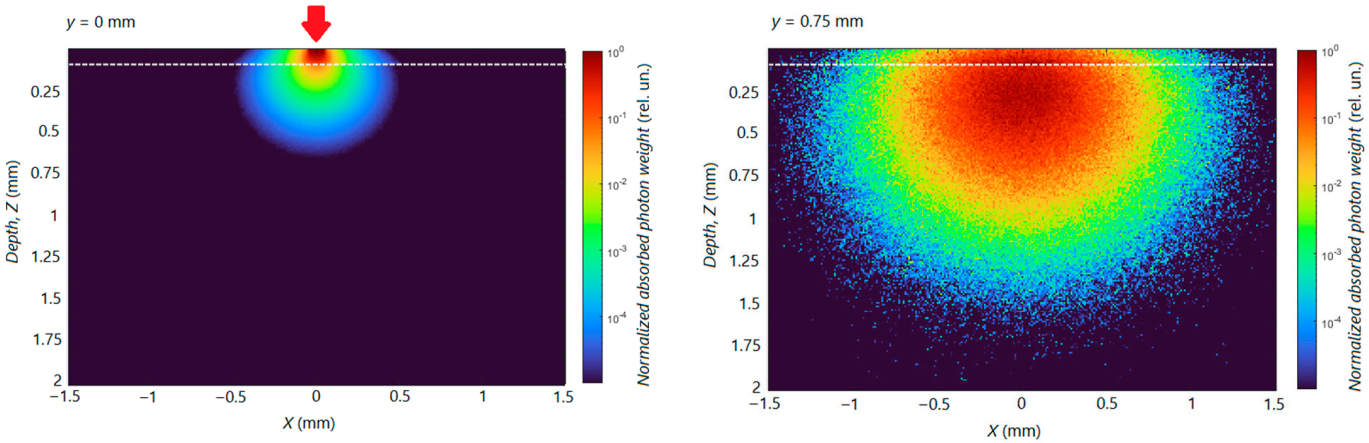

(**a**) (**b**)

Figure 3. Simulated distribution of absorbed UV radiation ($\lambda = 337$ nm) over two tissue cross-sections: (**a**) along the direction of the central axis ($y = 0$) of the irradiation spot; (**b**) at a distance of 0.75 mm from the central axis (or from the cross-section in (**a**)), $y = 0.75$ mm. The irradiation spot has a diameter $d = 100$ µm and is centered at $x = 0$, $y = 0$ (indicated with an arrow). A white dashed line indicates a boundary between the two layers.

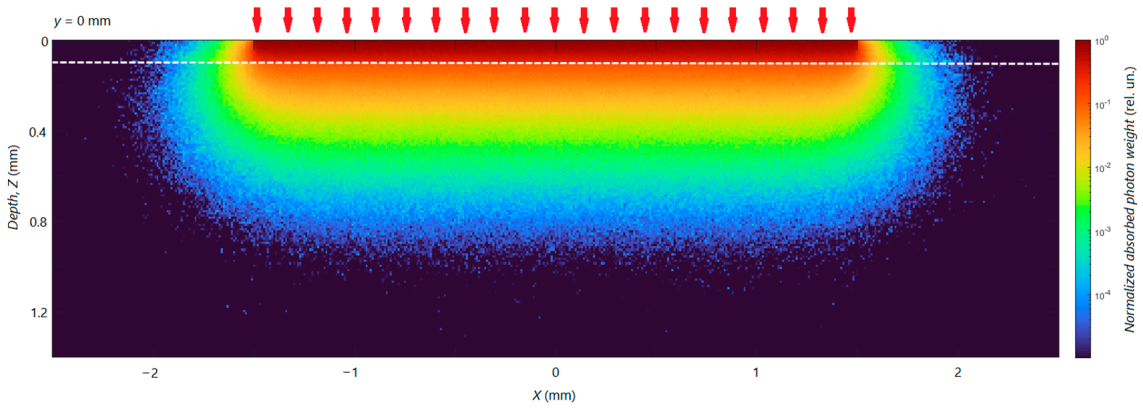

Figure 4. Simulated distribution of absorbed UV radiation (λ = 337 nm) over a central ($y = 0$) cross-section. The irradiation spot has a diameter $d = 3$ mm and is centered at $x = 0$, $y = 0$. A white dashed line indicates a boundary between the two layers.

Figure 4 shows the distribution of absorbed UV radiation under the irradiation spot with $d = 3$ mm (only the case of a central cross-section is shown). Here, the maximum absorption again occurs directly in the area under the irradiation spot. However, looking at Figures 3 and 4, differences in the propagation (and absorption) of UV radiation under irradiation spots of different sizes also become apparent. Namely, in the case of a small-diameter spot with $d = 100$ µm (which can be a fiber source in a real experiment), a significant portion of light propagates over distances greater than the spot's diameter and is absorbed in a region beyond the skin's area directly illuminated. In the case of an irradiation spot with a significantly larger diameter $d = 3$ mm, the size of the tissue region where diffuse light absorption is still significant is much smaller than the region limited by the projection of the irradiation spot. In particular, in the cylindrical region under

the tissue surface, limited by the projection of a small-diameter spot, we have only ~55% absorbed light of the total radiation absorbed in the tissue. In the case of a large-diameter irradiation spot, this value is ~98%; i.e., almost all radiation is absorbed in the geometric region directly under the spot. This fraction is above 99% for irradiation spot diameters $d > 7$ mm and reaches ~100% (above 99.5%) for $d = 1.4$ cm. It should be noted that the main part of absorption occurs in the first layer—the epidermis. Due to the strong diffusion of radiation in the dermal layer, the area where significant absorption occurs is much larger.

To better demonstrate the effect of light diffusion on the size of the tissue region in which light propagates, and to show the need to take diffusion into account when estimating the absorbed fraction of radiation, we calculated the volume V_α in which the bulk of radiation in the skin is absorbed ($\alpha = 0.95$) as a function of the irradiation spot size. Figure 5a plots the dependence of V_{95} on the area of the irradiation spot S for various values of S. In the upper inset of Figure 5a, for perception convenience, the dependence of V_{95} on the spot diameter d is also plotted. Figure 5a shows that the dependence $V_{95}(S)$ turns out to be linear (the dependence $V_{95}(d)$ is quadratic) only at relatively high values of S (or d). In this case, the area of light diffusion turns out to be much smaller than the geometric area of the tissue, limited by the size of the irradiation spot, and does not lead to a significant deviation of the shape of this area from cylindrical with the base of the cylinder coinciding with the irradiation spot on the skin surface. Note that as the spot size tends to zero, the volume V_α remains finite. This is clearly visible in the inset of Figure 5a, which shows an enlarged area of the $V_{95}(S)$ graph for small S. Even with $S = 0$ (pencil-like-beam spot), $V_\alpha \neq 0$. In particular, in the case in Figure 5a, the minimum possible volume at $\alpha = 95\%$ is $V_{\min,95} = V_{95}(S = 0) = 4.3 \cdot 10^{-2}$ mm^3.

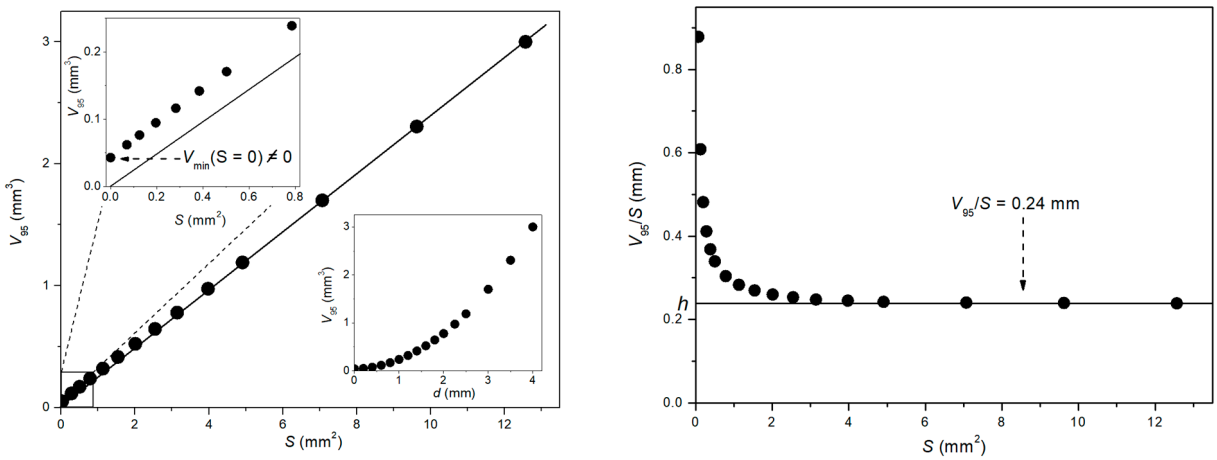

Figure 5. (**a**) The dependence of the tissue volume V_{95} in which 95% of absorbed light (λ = 337 nm) is accumulated on the irradiation spot area S; the solid line indicates the linear dependence at large S; the upper inset shows the enlarged region in the vicinity of $S = 0$; the bottom inset shows the dependence of V_{95} on the irradiation spot's diameter d. (**b**) The dependence of the ratio V_{95}/S on S; the solid line indicates the constant level of the ratio at large S.

Figure 5b plots the dependence of the ratio V_{95}/S on S. As S increases from zero, V_{95}/S decreases from "+∞" and at relatively large irradiation spot sizes reaches a constant level. In Figure 5b, this level, indicated by the dotted line, is $h = 0.24$ mm. Since the size of the area of light diffusion at large S is insignificant compared to the area of tissue limited by the projection of the irradiation spot, h actually represents the depth in tissue in which 95% of the absorbed radiation is concentrated. Similar calculations for λ = 315 nm gave $h = 0.18$ mm. Thus, UV radiation of the wavelengths studied does not penetrate deep into the dermis, which confirms the validity of using a two-layer skin model with a semi-infinite second layer within the framework of the problem under study.

By the degree of deviation of the V_{95}/S ratio from h, one can judge the limits of applicability of the conventional approach to assessing the absorbed dose, which neglects the diffusion of light and thus assumes the predominant absorption of light in the geometric region of the tissue limited by the irradiation spot contour. Having specified a certain value of the relative deviation of the ratio V_{95}/S from the value h, it is possible to enter the boundary values of the area S_{th} (and diameter d_{th}) of the spot, above which the use of the conventional approach is still permissible. Thus, for λ = 337 nm, a deviation of 10% and higher is achieved at values of S less than S_{th} = 1.54 mm^2 (corresponding diameter d_{th} = 1.4 mm). Similar results were obtained for λ = 315 nm due to the not very significant difference in the optical properties and h values. In general, we can talk about areas of UV irradiation spots of the order of 1.5–3 mm^2, beyond which the calculation of the dose as radiant exposure will not introduce a significant error. In the case of round spots, this corresponds to diameters of 1.4–2 mm.

3.4. Experimental Validation of Theoretical Calculations

Dose assessment in the conventional way, i.e., as the surface power area, in the case of irradiation spots of a small area (less than S_{th}), can lead to significant inaccuracies in the assessment of parameters of diagnostic and therapeutic procedures. In this work, we demonstrate this experimentally by estimating the time required to achieve erythema when the skin is irradiated with UV radiation using a fiber source with a diameter of 100 μm, located in close contact with the skin surface. This experiment actually serves as a validation of the calculations and conclusions made.

First of all, we should theoretically compare how long it will take to achieve erythema with a fiber source, if we use the MED value $D_{S,MED}$, defined as surface energy density (J/cm^2) (surface approach), and $D_{V,MED}$, calculated as volumetric density energy (J/cm^3) (volumetric approach) based on the obtained results of numerical simulations. The $D_{S,MED}$ values known from the literature are usually assessed when a UV radiation spot of a relatively large area is formed on the skin. In particular, various patches with a set of windows of equal size are often used, e.g., Daavlin DosePatch (Daavlin Company, Bryan, OH, USA), the square window of which is characterized by a side of 1.9 cm. At the same time, according to MC simulation results, in the case of a large-area irradiation spot (with $S > S_{th}$), we can assume that absorption occurs in a geometric region of depth h limited by the projection of the spot. In particular, for λ = 337 nm, 95% of absorbed radiation is concentrated in a region h = 0.24 mm deep under the spot. Using this, we determine the value of $D_{V,MED}$ according to (2) with $V_\alpha = S \cdot h$, which is valid for large irradiation spots. The fraction of absorbed UV radiation A in (2) is nearly 0.84 in the case of the reflection-index-mismatched boundary for λ = 337 nm and independent of the irradiation spot's size as obtained by MC simulations. For α = 0.95, we obtain $D_{V,MED}$ = 795 J/cm^3, using $D_{S,MED}$ = 23.8 J/cm^2 as a reference.

In the in vivo experiment, the surface power density of radiation with λ = 337 nm at the output of the fiber source (19 fibers with a diameter of 100 μm) is ~1.55 W/cm^2. The volumetric power density created in the tissue on average and, accordingly, D_V can be estimated using the volume to which the main part of the radiation is absorbed (V_{95}). According to the simulation results, $V_{95} = 4.5 \cdot 10^{-5}$ cm^3 for one fiber with d = 100 μm; A = 0.87 for the reflection-index-matched boundary.

Table 2 shows calculated values D_S and D_V for a set of different t values; the values where the MED is exceeded are highlighted in bold. When using the surface approach to calculate the dose, the MED is already exceeded during the first 15 s of skin exposure to UVA light through a fiber probe. The volumetric approach gives an exposure duration of ~360 sec (6 min) to achieve erythema.

Table 2. Calculated values of D_S and D_V for light with a wavelength of 337 and 315 nm emitted by the fiber probe (19 fibers with a diameter of 100 μm) with a power of 2.3 mW (λ = 337 nm) and 70 μW (λ = 315 nm). Values that exceed the MED are highlighted in bold.

Time (sec)	λ = 337 nm		λ = 315 nm	
	D_S (J/cm^2)	D_V (J/cm^3)	D_S (J/cm^2)	D_V (J/cm^3)
5	7.7	11.2	0.2	0.6
20	**31.0**	44.7	**0.9**	2.4
100	**154.8**	223.3	**4.7**	12.0
200	**309.6**	446.6	**9.4**	24.0
400	**619.2**	**893.2**	**18.8**	**48.0**

Figure 6 shows a photograph of the forearm area of a healthy volunteer irradiated with UVA radiation with a wavelength of 337 nm using a fiber probe of the Multicom system. The photograph was taken 24 h after irradiation. The areas where the distal end of the probe was held on the skin surface are marked with a marker. Numbers 1–10 in Figure 6 correspond to irradiation durations of 30–300 s in increments of 30 s. Erythema in the form of a clear ring (19 fibers in the probe are arranged in a circle) was found in the area where the irradiation duration was 300 s (5 min)—see the inset in Figure 6. This result turns out to be quite close to the predictions made within the volumetric approach (~360 sec).

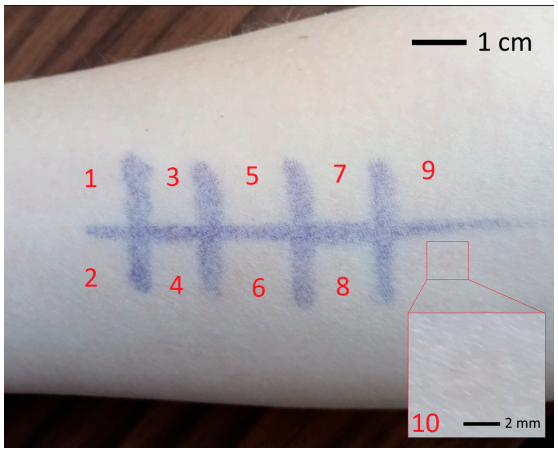

Figure 6. Photograph of the forearm area of a healthy volunteer irradiated with 337 nm UVA light using a fiber probe. Numbers 1–10 correspond to irradiation durations of 30–300 s in increments of 30 s. The inset shows a magnified image of the area exposed to irradiation for 300 sec.

Similar results were obtained for UVB radiation (λ = 315 nm). In this case, $D_{S,MED}$ = 0.87 J/cm^2, and recalculation into $D_{V,MED}$ based on the simulation results gives 40 J/cm^3 at α = 0.95. The surface power density of radiation with λ = 315 nm in our experiment is ~ 50 mW/cm^2. The calculation results for the time to reach the MED within the surface and volumetric approaches are also shown in Table 2 (V_{95} in this case is 2.6·10^{-5} cm^3 for one 100 μm diameter fiber). While the dose assessment as radiation exposure gives an excess of the MED value within 20 s (the output power of 315 nm radiation is much weaker than the 337 nm radiation in our experiment), the calculation based on the dose distribution in the tissue volume under the fiber gives 330 s before the MED is reached. In the in vivo experiment (observation after 24 h), erythema appeared in the skin zone irradiated for 420 s (7 min). The experimental value is again much closer to the predictions given by the volumetric approach than by the conventional surface approach.

Despite this, in the case of both wavelengths, an underestimation of the time to reach the MED is still observed compared to the in vivo experiment. There may be several reasons for the discrepancy between the experimentally obtained and calculated times. Among them, in particular, one can note the choice of α, which determines the fraction of absorbed

radiation that is taken into account in the calculations and possible inaccuracies in the selection of the optical properties of the skin. In addition, individual photosensitivity to UV light (the MED value) is determined by a complex of endo- and exogenous factors: the influence of local/systemic photosensitizing drugs, or drugs reducing sensitivity; skin phototype; anatomical area exposed; presence of tanning; gender; age; skin hydration; and the peculiarities of the functioning of the protective and reparative systems of the skin. Visually detectable UV erythema is the result of vasodilation in response to the release of vasoactive inflammatory mediators (e.g., cytokines) formed during primary and secondary alteration and death of target cells in the affected area. As a consequence, the characteristics of the reactivity of the vascular and immune systems, their neuroendocrine regulation and the concentration of protective pigments in the individual's skin determine the intensity of the inflammatory response. This leads to significant interindividual variability in MED values. In any case, already at this stage of research, the results obtained prove the correctness of using a volumetric approach to dose assessment (calculation of volumetric energy density) in the case of creating small-area irradiation spots on the skin surface, including when using radiation sources with small apertures (in particular, fibers).

The results obtained indicate the possibility of safely carrying out diagnostic procedures using UVA and UVB radiation for tens and even hundreds of seconds. Since a common diagnostic procedure using fiber probes lasts less than 30 s, one can even raise the incident radiation power and use fewer radiating fibers or light sources with smaller apertures.

4. Conclusions

Using MC simulations, we demonstrated the physical aspects of UV radiation transport in human skin depending on the size of the irradiation spot on the skin surface. The cases of UVA and UVB light were considered. Numerical results on the absorbed energy distribution in skin in the case of a small irradiation spot (~millimeter or less in size), showed that when calculating accumulated dose, it is necessary to take into account the volume where UV radiation is mainly absorbed. A dose estimated as a radiant exposure (J/cm^2) in this case turns out to be overestimated due to the small spot area and, as a consequence, the high radiation power density. As a result, the time to reach the MED turns out to be greatly underestimated. This, in turn, implies the impossibility of carrying out a long-term diagnostic UV procedure, including the use of optical fibers to deliver radiation to biological tissue. On the contrary, the calculation of volumetric energy density turns out to be correct in the case of irradiation spots of small area, which is confirmed by in vivo experiments when assessing the time required to achieve erythema. The main result of the work shows the possibility of safely performing in vivo skin diagnostics with UVA and UVB light for a sufficiently long time (using a relatively low power of the UV radiation source).

The use of the conventional approach to assessing the absorbed dose as radiant exposure turns out to be correct in the case of relatively large irradiation spots on the skin surface. In particular, within the framework of our theoretical approach, it is shown that in the case of a spot area greater than approximately 1.5–3 mm^2 (which corresponds to the round spot diameter of ~1.4–2 mm), the dose can be estimated as radiant exposure without introducing a significant error.

Author Contributions: Conceptualization, A.P.T. and D.A.R.; methodology, A.P.T. and D.A.R.; software, A.P.T.; validation, A.P.T., M.E.S. and D.A.R.; formal analysis, A.P.T. and M.E.S.; investigation, A.P.T. and M.E.S.; resources, A.P.T. and D.A.R.; data curation, A.P.T.; writing—original draft preparation, A.P.T. and M.E.S.; writing—review and editing, A.P.T., M.E.S. and D.A.R.; visualization, A.P.T.; supervision, A.P.T. and D.A.R.; project administration, A.P.T. and D.A.R.; funding acquisition, A.P.T. and D.A.R. All authors have read and agreed to the published version of the manuscript.

Funding: This research received no external funding.

Institutional Review Board Statement: The study protocol complies with the ethical principles of the Declaration of Helsinki (2013 revision) and was approved by the Independent Ethics Committee of the Moscow Regional Research and Clinical Institute ("MONIKI") (Protocol No. 16 of 15 December 2022).

Informed Consent Statement: Written informed consent was obtained from all participants.

Data Availability Statement: Data can be made available on request.

Conflicts of Interest: The authors declare no conflict of interest.

References

1. Moseley, H.; Allan, D.; Amatiello, H.; Coleman, A.; du Peloux Menagé, H.; Edwards, C.; Exton, L.S.; Ferguson, J.; Garibaldinos, T.; Martin, C.; et al. Guidelines on the measurement of ultraviolet radiation levels in ultraviolet phototherapy: Report issued by the British Association of Dermatologists and British Photodermatology Group 2015. *Br. J. Dermatol.* **2015**, *173*, 333–350. [CrossRef]
2. Herzinger, T.; Berneburg, M.; Ghoreschi, K.; Gollnick, H.; Hölzle, E.; Hönigsmann, P.; Lehmann, P.; Peters, T.; Röcken, M.; Scharffetter-Kochanek, K.; et al. S1-Guidelines on UV phototherapy and photochemotherapy. *J. Dtsch. Dermatol. Ges.* **2016**, *14*, 853–876. [CrossRef]
3. Makmatov-Rys, M.B.; Kulikov, D.A.; Kaznacheeva, E.V.; Khlebnikova, A.N. Pathogenic features of acute ultraviolet-induced skin damage. *Russ. J. Clinic. Dermatol. Venereol.* **2019**, *18*, 412–417. (In Russian) [CrossRef]
4. IAEA. Absorbed Dose Determination in External Beam Radiotherapy. In *Technical Reports Series No. 398*; IAEA: Vienna, Austria, 2000; p. 229.
5. Almond, P.R.; Biggs, P.J.; Coursey, B.M.; Hanson, W.F.; Huq, M.S.; Nath, R.; Rogers, D.W. AAPM's TG-51 protocol for clinical reference dosimetry of high-energy photon and electron beams. *Med. Phys.* **1999**, *26*, 1847–1870. [CrossRef]
6. Lehnen, M.; Koppermann, M.; Korber, A.; Grabbe, S.; Dissemond, J. Vergleich der minimalen Erythemdosis von Schmalspektrum-UV-B-und Breitspektrum-UV-B-Strahlern mit einem neuen UV-Handgerät. *Hautarzt* **2005**, *56*, 258–264. [CrossRef]
7. Gambichler, T.; Majert, J.; Pljakic, A.; Rooms, I.; Wolf, P. Determination of the minimal erythema dose for ultraviolet A1 radiation. *Br. J. Dermatol.* **2017**, *177*, 238–244. [CrossRef]
8. Yun, S.; Kwok, S. Light in diagnosis, therapy and surgery. *Nat. Biomed. Eng.* **2017**, *1*, 0008. [CrossRef]
9. Tuchin, V.V.; Utz, S.R.; Yaroslavsky, I.V. Tissue optics, light distribution, and spectroscopy. *Opt. Eng.* **1994**, *33*, 3178–3188. [CrossRef]
10. Yurii, P.; Sinichkin, Y.P.; Utz, S.R.; Mavliutov, A.H.; Pilipenko, H.A. In vivo fluorescence spectroscopy of the human skin: Experiments and models. *J. Biomed. Opt.* **1998**, *3*, 201–211. [CrossRef]
11. Throm, C.M.; Wiora, G.; Reble, C.; Schleusener, J.; Schanzer, S.; Karrer, H.; Kolbe, L.; Khazaka, G.; Meinke, M.C.; Lademann, J. In vivo sun protection factor and UVA protection factor determination using (hybrid) diffuse reflectance spectroscopy and a multi-lambda-LED light source. *J. Biophotonics* **2020**, *14*, e202000348. [CrossRef]
12. Utzinger, U.; Richards-Kortum, R.R. Fiber optic probes for biomedical optical spectroscopy. *J. Biomed. Opt.* **2003**, *8*, 121–147. [CrossRef]
13. Kulikov, D.; Makmatov-Rys, M.; Raznitsyna, I.; Glazkova, P.; Gerzhik, A.; Glazkov, A.; Andreeva, V.; Kassina, D.; Rogatkin, D. Methods of Non-Invasive In Vivo Optical Diagnostics in the Assessment of Structural Changes in the Skin Induced by Ultraviolet Exposure in an Experimental Model. *Diagnostics* **2021**, *11*, 1464. [CrossRef]
14. Parrish, J.A.; Jaenicke, K.F.; Anderson, R.R. Erythema and melanogenesis action spectra of normal human skin. *Photochem. Photobiol.* **1982**, *36*, 187–191. [CrossRef]
15. Raznitsyna, I.A.; Tarasov, A.P.; Rogatkin, D.A. An improved system for in vivo fluorescent analysis in medicine. *Instrum. Exp. Tech.* **2020**, *63*, 267–272. [CrossRef]
16. Tarasov, A.P.; Raznitsyna, I.A.; Shtyflyuk, M.E.; Rogatkin, D.A. Is the Minimal Erythema Dose Achievable at Optical Spectroscopy of Skin in Vivo? In Proceedings of the 2023 IEEE Radiation and Scattering of Electromagnetic Waves, Divnomorskoe, Russia, 26–30 June 2023; pp. 340–343. [CrossRef]
17. Prahl, S.A.; Keijzer, M.; Jacques, S.L.; Welch, A.J. A Monte Carlo model of light propagation in tissue. *Dosim. Laser Radiat. Med. Biol.* **1989**, *10305*, 105–114.
18. Wang, L.; Jacques, S.L.; Zheng, L. MCML—Monte Carlo modeling of light transport in multi-layered tissues. *Comput. Meth. Programs Biomed.* **1995**, *47*, 131–146. [CrossRef]
19. Bruls, W.A.; Slaper, H.; van Der Leun, J.C.; Berrens, L. Transmission of human epidermis and stratum corneum as a function of thickness in the ultraviolet and visible wavelengths. *Photochem. Photobiol.* **1984**, *40*, 485–494. [CrossRef]
20. Patwardhan, S.V.; Dhawan, A.P.; Relue, P.A. Monte Carlo simulation of light-tissue interaction: Three-dimensional simulation for trans-illumination-based imaging of skin lesions. *IEEE Trans. Biomed. Eng.* **2005**, *52*, 1227–1236. [CrossRef]
21. Nielsen, K.P.; Zhao, L.; Juzenas, P.; Stamnes, J.J.; Stamnes, K.; Moan, J. Reflectance Spectra of Pigmented and Nonpigmented Skin in the UV Spectral Region. *Photochem. Photobiol.* **2004**, *80*, 450–455. [CrossRef]
22. Salomatina, E.; Jiang, B.; Novak, J.; Yaroslavsky, A.N. Optical properties of normal and cancerous human skin in the visible and near-infrared spectral range. *J. Biomed. Opt.* **2006**, *11*, 064026. [CrossRef]
23. Jacques, S.L. Optical properties of biological tissues: A review. *Phys. Med. Biol.* **2013**, *58*, R37–R61. [CrossRef]

24. Friebel, M.; Roggan, A.; Müller, G.J.; Meinke, M.C. Determination of optical properties of human blood in the spectral range 250 to 1100 nm using Monte Carlo simulations with hematocrit-dependent effective scattering phase functions. *J. Biomed. Opt.* **2006**, *11*, 034021. [CrossRef]
25. Bosschaart, N.; Edelman, G.J.; Aalders, M.C.; van Leeuwen, T.G.; Faber, D.J. A literature review and novel theoretical approach on the optical properties of whole blood. *Lasers Med. Sci.* **2014**, *29*, 453–479. [CrossRef]